Available online at www.sciencedirect.com
SCIENCE DIRECT®
Coordination Chemistry Reviews 248 (2004) 1455–1468
COORDINATION CHEMISTRY REVIEWS
www.elsevier.com/locate/ccr

Review

Polymers in dye sensitized solar cells: overview and perspectives

A.F. Nogueira, C. Longo, M.-A. De Paoli*

Laboratório de Polímeros Condutores e Reciclagem, Instituto de Química, Unicamp, C.P. 6154, 13084-971 Campinas, São Paulo, Brazil

Received 17 October 2003; accepted 7 May 2004
Available online 6 August 2004

Contents

Abstract

Dye sensitized solar cells (DSSC) are the result of a combination of several different materials: optically transparent electrodes, nanoparticulated semiconductors, coordination compounds, inorganic salts, solvents and metallic catalysts. Each material performs a specific task toward the overall objective of harvesting solar light and transforming it into electricity. To improve the efficiency and increase the technological perspectives of DSSC, there is a tendency to substitute some of these materials by polymers. Poly(ethylene terephthalate) based electrodes can substitute glass electrodes, improving the flexibility and impact resistance of a DSSC. Liquid electrolytes are volatile and may leak if the cell is not properly sealed. Their replacement by polymeric electrolytes solves both problems with the additional advantage that they act as a binder for the electrodes. More recently, intrinsically conducting polymers have been used as hole conducting materials in DSSC, with promising results. In this review we will discuss these tendencies, highlighting the advantages of using polymers, and discussing the problems faced by researchers working in this area.

Keywords: Solid-state dye sensitized cell; Polymer electrolytes; Polymer electrodes; Conducting polymers

1. Introduction

Dye sensitized solar cells (DSSC) or "Grätzel cells" have attracted considerable interest in the scientific community due to their low energetic production cost, low cost of the raw materials and high efficiency to convert solar energy into electricity [1–4]. These cells achieve 10.4% certified solar power efficiencies [5] and their stability data indicates, at least, 10 years of use in outdoor applications [6]. The efficiency of a DSSC is lower than the classical crystalline silicon cells and the next generation of solid-state thin films technology such as CIGS cells. However, DSSC technology presents lower costs and, since we still are far from the theoretical efficiency, there is a high potential for improvements in efficiency to be developed.

Energy conversion in a DSSC is based on the injection of an electron from a photoexcited state of the sensitizer dye (typically a bipyridine metal complex) into the conduction band of the nanocrystalline semiconductor (TiO_2 is by far the most employed oxide semiconductor), as depicted in Fig. 1. These cells also employ a liquid electrolyte (usually an iodide/triiodide redox-active couple dissolved in an or-

* Corresponding author. Tel.: +55 19 3788 3075; fax: +55 19 3788 3023.
E-mail address: mdepaoli@iqm.unicamp.br (M.-A. De Paoli).

0010-8545/$ – see front matter © 2004 Elsevier B.V. All rights reserved.
doi:10.1016/j.ccr.2004.05.018

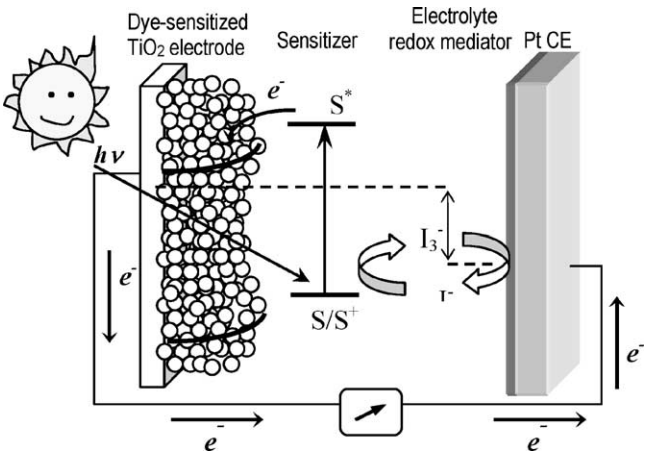

Fig. 1. Schematic representation of a dye-sensitized TiO_2 solar cell (DSSC) and the electron transfer processes involved in energy conversion (S represents the dye sensitizer and I^-/I_3^- is the charge mediator).

ganic solvent) to reduce the dye cation (viz., regenerate the ground state of the dye). Regeneration of iodide ions, which are oxidized in this reaction to triiodide, is achieved at a platinised counter electrode, Eqs. (1)–(6):

$$TiO_2|S + h\nu \rightarrow TiO_2|S^* \quad (1)$$

$$TiO_2|S^* \rightarrow TiO_2|S^+ + e_{cb}^- \quad (2)$$

$$TiO_2|S^+ + e_{cb}^- \rightarrow TiO_2|S \quad (3)$$

$$TiO_2|S^+ + \tfrac{3}{2}I^- \rightarrow TiO_2|S + \tfrac{1}{2}I_3^- \quad (4)$$

$$\tfrac{1}{2}I_3^- + e_{(Pt)}^- \rightarrow \tfrac{3}{2}I^- \quad (5)$$

$$I_3^- + 2e_{cb}^- \rightarrow 3I^- \quad (6)$$

In summary, these cells are the result of a combination of several different materials: optically transparent conducting electrodes (used to deposit the oxide layer and the metallic catalysts, acting as photoanode and counter electrode, respectively), nanoparticulated oxide semiconductors, inorganic metal complexes or organic dyes (as sensitizers), inorganic salts (in the electrolyte), solvents and metallic catalysts. Each material performs a specific task in the complex mechanism of a DSSC and contributes to the overall solar cell efficiency [7].

To improve the efficiency and increase the technological perspectives of a DSSC, first, each component must be carefully improved/modified separately. In the last decade, there has been a tendency to replace some of these materials by polymers. This tendency is not exclusive for the DSSC, but a general tendency in other research fields involving optic and electronic materials. Plastic materials, when properly modified, combine the excellent processing advantages and mechanical properties of conventional polymers with the desired electrical, optical, electronic and magnetic properties of metals and semiconductors. The replacement of some DSSC components by plastic ones is not only related to modernization, but is also based on some problems found with these cells, so that they might become a competitive technology on the market. In this review we will discuss these new tendencies separately, highlighting the advantages of the use of polymers, and discuss the problems faced by researchers working in this area.

2. Plastic electrodes based on PET

The use of glass electrodes brings restrictions related to fragility and shape limitations. Several advantages can be obtained replacing the usual conducting glass substrates by plastic electrodes. These are related to their lower weight, increased flexibility, higher impact resistance and lower cost. Besides, the use of flexible substrates opens up the possibility to manufacture DSSC using a continuous roll-to-roll, high speed coating process and design prototypes in different shapes to be applied at different surfaces (e.g. glass windows). In addition, the ability to produce DSSC in continuous steps would substantially lower the cost of the cells compared to the batch process used for glass-based cells.

Motivated by these technological advantages, the research for developing flexible and solid-state electrochromic [8–10] and photoelectrochemical devices [11–14] has received considerable attention. This became possible after the large-scale production of flexible transparent electrodes, like films of poly(ethylene terephtalate) coated with indium doped tin oxide (ITO–PET) from IST, Belgium. Several groups have used these plastic substrates in DSSC with interesting results [10–19]. Presently, the efficiencies of cells using ITO–PET electrodes are lower than those of the classical cell using glass substrates. However, efficiencies of 5.5% have been reported for a complete solid-state version of DSSC using plastic electrodes [16,20].

The major drawback involved in developing “plastic” DSSC concerns the deposition of the TiO_2 film. In the traditional batch process, a colloidal TiO_2 suspension is deposited onto a glass substrate by blade coating or screen-printing procedures. After this, the films are annealed at high temperatures, 450 °C for 30 min. This sintering step removes the binder and solvent, giving rise to an electrically-connected network of TiO_2 particles. However, with ITO–PET electrode, the thermal treatment is limited to 150 °C, because above this temperature the polymer undergoes thermal degradation, loosing its transparency and becoming completely distorted. As a consequence, TiO_2 film deposition on ITO–PET at 150 °C results in poor adhesion, reduced electrical contact between the particles and low dye adsorption. Another issue is that the low annealing temperature precludes the total elimination of organic residues from the surfactants commonly used in TiO_2 suspensions [14,19].

Several groups are focusing their efforts into developing plastic DSSC by modifying the traditional batch process or by introducing new methods for TiO_2 synthesis and/or

deposition. Pichot et al. have demonstrated the possibility to make plastic DSSC by applying a low sintering temperature (100 °C) to TiO_2 colloidal films in the absence of organic surfactants [10,20]. Cells assembled using films deposited from TiO_2 suspensions containing surfactant and heated at high temperatures present IPCE values higher than cells prepared with films obtained at low temperature. However, the latter films have a larger internal surface area and can therefore absorb more dye for the same film thickness.

Tripathy and coworkers have discovered an alternative method to interconnect the TiO_2 particles at low temperature by heating a suspension of TiO_2 and a titanium alkoxide at 150 °C for 1 h [21]. More recently, this process has been modified in such a way that the suspension coated on PET–ITO films required heating to 110 °C for <1 min [22]. These authors claim to produce plastic cells (area = 0.5 cm^2) exhibiting efficiencies higher than 5% at air mass 1.5 condition (AM 1.5), and estimated that the manufacturing cost could be as low as the lowest estimated cost for amorphous and crystalline silicon [23]. In the same direction, a highly efficient flexible DSSC prepared on a conductive plastic film substrate was assembled using mechanically stable mesoporous nanocrystalline TiO_2 films prepared at low temperature (100 °C) by hydrothermal treatment [24]. These authors used an aqueous paste containing nanocrystalline TiO_2 powder and titanium salts. The latter are converted into crystalline TiO_2, which acts as a "glue" to chemically connect the originally present TiO_2 particles [24].

A very successful alternative method for preparation of a nanoporous semiconductor film onto ITO–PET substrate at room temperature was first proposed by Hagfeldt and collaborators from the Ångström Solar Center in Upsala, Sweden [15]. They used a pressing technique that consist in statically or continuously pressing powder films of TiO_2 (*Degussa P-25*), previously dispersed in ethanol, onto a glass or plastic substrate. A typical pressure for preparing efficient solar cells is 1000 kg cm^{-2} for few seconds. The continuous method is only applied to the plastic substrate. Interestingly, films prepared by the traditional annealing technique and films prepared from the pressing technique present the same mechanical and morphological properties and porosity. The DSSC assembled using compressed films with an additional heat treatment ("annealed") and with compressed films not further treated ("non-annealed") on glass substrates exhibit similar performance. When the glass is replaced by a conducting plastic substrate, surprising results were obtained for an all-plastic sandwich cell. In this cell the counter electrode consisted of platinized SnO_2 powder pressed on a conducting plastic substrate. The electrode was produced without heat treatment. The overall cell efficiency (active area of 0.32 cm^2) was 4.9% at 10 mW cm^{-2}. Because of the series resistance losses in the conducting plastic layer (IST, sheet resistance: 60 Ω per square) it was very difficult to reach high conversion efficiencies with pressed SnO_2 electrodes at higher light intensities. Nevertheless, at 100 mW cm^{-2} intensity, they attained 0.41 for the fill factor, FF at an open-circuit voltage, V_{OC}, of 0.76 V, short-circuit current, I_{SC} = 7.3 mA cm^{-2} and overall efficiency, η = 2.3%. In another study, the same authors have explored alternatives to improve the efficiency of the all-plastic sandwich cell using the same pressing technique [16]. Plastic cells with overall efficiencies of 5.5% were obtained. However, their stability was poor, which was associated to the permeability of the ITO–PET substrate to water and other small molecules. It is important to point out that, in these studies, all plastic DSSC have employed a liquid electrolyte (typically I_3^-/I^- in acetonitrile) and problems with solvent leaking and cell integrity during long exposure remained unsolved.

Our research group has employed polymer electrolytes based on ethylene oxide copolymers complexed with lithium or sodium iodide as promising candidates to replace the liquid electrolyte (a complete description of polymer electrolytes will be given in a subsequent section). Using conducting plastic substrates and replacing the liquid electrolyte by the polymer electrolyte a complete "plastic solar cell" was assembled. The first attempt to develop such cells using Ru^{II}(2,2′-bipyridyl-4,4′-dicarboxylate)$_2$-$(NCS)_2$ (also called N3 dye) as sensitizer, produced devices (active area = 1 cm^2) with I_{SC} = 0.40 mA cm^{-2}, V_{OC} = 0.72 V, FF = 0.42 and η = 0.12% under 100 mW cm^{-2} (η = 0.22% under 10 mW cm^{-2}). It is clear from the low FF values that the series resistance plays an important role when assembling complete plastic devices. This assumption was confirmed by electrochemical impedance spectroscopy [14,17–19].

Another alternative to make flexible DSSC, introduced by our group, consists of depositing a film of TiO_2 particles onto flexible electrodes (ITO–PET) from the usual suspension, exposing the film to UV radiation for a few minutes and heating at 140–150 °C [19]. The UV treatment promotes the photodegradation of organic compounds, allowing the elimination of most of the organic residues from the TiO_2 suspension. The resulting films were mechanically stable, presented an intense adsorption of the dye and relatively good performance in solid-state, flexible DSSC assembled with a polymer electrolyte. These plastic cells, with an active area of 1 cm^2, exhibited short-circuit current I_{SC} = 0.54 mA cm^{-2}, open circuit potential V_{OC} = 0.80 V and η = 0.23% under 100 mW cm^{-2} (η = 0.32% under 10 mW cm^{-2}). Typical *I–V* curves under different light intensities are shown in Fig. 2. The efficiency of these cells also decayed with time. Cell performance loss was associated with an increase in the series resistance of the cell, as verified by monitoring the I_{SC} and V_{OC} together with electrochemical impedance measurements, as a function of time [19]. This effect was not so evident for cells prepared by a similar procedure using glass electrodes, suggesting that the flexible electrode creates a large series resistance in the solar cell. Although the overall conversion efficiency is low, in comparison to DSSC using glass electrodes, the recent advances on this topic can be considered very promising.

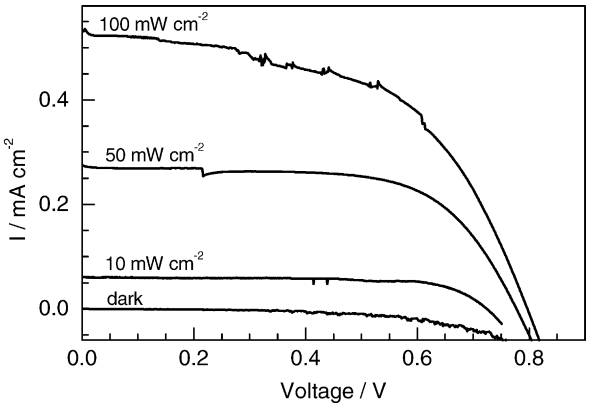

Fig. 2. Typical *I–V* curves obtained at different light intensities for an N3 dye sensitized TiO_2 solar cell assembled with P(EO–EPI)/I^-/I_3^- polymer electrolyte and using ITO–PET as plastic electrodes.

3. Liquid electrolytes

The redox couple present in the electrolyte is of crucial importance for stable operation of a DSSC, transporting the charge between the photoanode and the counter electrode during regeneration of the dye. After electron injection, the oxidized dye must be re-reduced to its ground state as fast as possible by the electron donor in the electrolyte. Thus, the choice of the charge mediator should take into account the dye redox potential, which must be suitable for its efficient regeneration. Also, the redox couple must be fully reversible and should not exhibit significant absorption of light in the same spectral region as the dye. Another important requirement is related to the solvent, which should permit the fast diffusion of charge carriers, while not causing the desorption of the dye from the oxide surface [7,25,26]. The redox couple in the electrolyte influences the reduction of the oxidized state of the dye as well as the other processes in the DSSC, including electron-transfer kinetics at the counter-electrode, dark current reactions, ion-pairing with the dye and also charge transport in the semiconductor film and in solution [27].

A very important parameter for stable operation of the cell and maximum solar power output is related to the mass transport of charge carriers in the electrolyte, which occurs by diffusion. This process will depend not only on the diffusion coefficient of the ions and viscosity of the solvent, but also on the structure of the porous film electrode. The apparent triiodide diffusion coefficient in acetonitrile using a TiO_2 membrane with a porosity of 55% is ca. $3.4 \times 10^{-6}\,cm^2\,s^{-1}$. This value is one order of magnitude lower than the free diffusion of triiodide in the same solvent (at 25 °C). Thus, the diffusion of the electroactive species can be obstructed in porous TiO_2 films. In a DSSC, this effect can be particularly critical at high light intensities, when large current densities pass through the cell [28]. In fact, it is well known that DSSC are much more efficient under low light levels.

The electrolyte composition also affects the photovoltage (V_{OC}) of the DSSC, which is the difference between the Fermi level of the semiconductor and the electrochemical potential of the redox pair. Furthermore, the photovoltage can also be affected by non-electroactive species in the electrolyte, particularly by small cations such as protons, Li^+, etc. These species can adsorb or intercalate onto the surface of the TiO_2 oxide, shifting its conduction band edge to a lower energy level. This can lower the photovoltage, but enhances the efficiency of interfacial charge injection, increasing the photocurrent and the overall efficiency of the DSSC [28–30].

The most used charge mediator in DSSC consist of the iodide (I^-)–triiodide (I_3^-) redox couple (derived from I^- and I_2), since it exhibits an electrochemical redox potential suitable for reduction of several oxidized dyes and the best kinetic properties. However, since triiodide solutions are colored and present absorption bands in the visible region, high concentrations may reduce light absorption by the dye. Moreover, I_3^- ions can react with injected electrons (Fig. 1), Eq. (6) and high concentrations increase the dark current. Thus, the concentration of I^-/I_3^- must be optimized [28,29]. However, this redox pair is not adequate to regenerate the ground state of some dyes, such as the Os(II) bipyridiyl sensitizers, which need stronger reducing agents [31,32].The application of other charge mediators with different electrochemical potentials was also investigated, for instance the redox couples $(SeCN)_2/SeCN^-$ and $(SCN)_2/SCN^-$ dissolved in acetonitrile. These redox couples present a more positive equilibrium potential than the I_3^-/I^- redox pair, however, the photopotential of the DSSC does not increase as expected, and the cells present lower efficiencies. From transient absorption spectroscopy, it was demonstrated that the lower efficiencies were related to a slower dye regeneration rate when SCN^- or $SeCN^-$ were used instead of I^- [27]. More recently, Bignozzi and co-workers [33] have used a mixture of Co(II) and Co(III) complexes of substituted bipyridine ligands as possible alternatives to the I_3^-/I^- pair. They also investigated the role of different counter electrode substrates, such as gold, platinum and carbon. Although the cell efficiency is lower when compared to the I_3^-/I^- pair, the authors have achieved IPCE values of 80% for tris(4,4′-di-*tert*-butyl-2,2′-dipyridyl)-cobalt(II/III)perchlorate as redox pair.

As previously mentioned when discussing the electrolyte in DSSC, it is worthwhile to consider the sealing, necessary to prevent the loss of the liquid electrolyte by leakage and/or evaporation of the solvent. Thus, liquid junction DSSC need a perfect seal, with a binder that must be chemically resistant to the electrolyte (usually an organic solvent containing the corrosive I_3^-/I^- redox couple). The use of a liquid electrolyte is the major factor retarding the commercial development of DSSC. Several attempts have been made to find a suitable substitute, such as room temperature molten salts based on imidazolium and pyridinium, organic and inorganic hole transporting materials (HTM) and polymer based elec-

trolytes. In the next sections, we will outline the most recent advances in the substitution of the liquid electrolyte by polymer-based electrolytes, such as intrinsically conducting polymers, gel and solid-state polymer electrolytes.

4. Conducting polymers as HTM materials

A scientifically interesting and promising approach to replace the liquid electrolyte in DSSC consists in the use of p-type semiconductors, referred as hole transporting materials. In principle, all materials with p-type semiconducting behavior, capable of accepting holes from the dye cation, are potential candidates to replace the liquid electrolyte in DSSC. These materials can be crystalline inorganic salts, such as CuI and CuSCN, or organic molecular solids and polymers, such as those based on the triarylamine derivatives 2,2′,7,7′-tetrakis(*N*,*N*-di-*p*-methoxy-phenylamine)-9,9′-spirobifluorene (Spiro-MeOTAD) [34] and the (*N*,*N*-9-diphenyl-*N*,*N*-9-bis(3-methylphenyl)4,49-diamine (TPD) [35–37]. The focus of this review is on the more recent advances made in the field of polymeric HTM applied to DSSC.

The cell mechanism using HTM is analogous to liquid or polymer electrolyte DSSC. After dye excitation and electron transfer to the conduction band of TiO_2, the ground state of the dye is regenerated by the HTM: electrons from the highest occupied molecular orbital (HOMO) of the HTM regenerate the ground state of the dye molecules instead of the redox couple of the electrolyte. The oxidized HTM material is then reduced at the counter electrode (e.g. a nanometer thick thin-layer of gold). The main difference relies on the kind of transport between the electrodes. In the cell using HTM, the transport is typically electronic, in comparison to ionic transport in the DSSC using liquid or polymer electrolyte. Eqs. (7)–(11) show the most important reactions involved in a DSSC using a HTM. In the solid-state DSSC version, the charge transfer reactions at the dye-sensitized nanocrystalline TiO_2–HTM interface play a key role in determining the overall solar cell efficiency.

$$S* \rightarrow S^+ + e^-(TiO_2) \quad (7)$$

$$S^+ + HTM \rightarrow S + HTM^+ \quad (8)$$

$$HTM^+ + e^-(\text{Al or Au}) \rightarrow HTM \quad (9)$$

$$S^+ + e^-(TiO_2) \rightarrow S \quad (10)$$

$$e^-(TiO_2) + HTM^+ \rightarrow HTM \quad (11)$$

Intrinsically conducting polymers are well known as good hole transporting material, carrying current densities of several mA cm^{-2} [38,39]. Thus, these materials are potential candidates to use as HTM in solid-state DSSC. Fig. 3 depicts the chemical structures of the repeating units of some conducting polymers. These materials are commonly known as "synthetic metals" because they possess the electrical, electronic, magnetic and optical properties of a metal or a semiconductor, while retaining the mechanical properties of conventional polymers. Besides, they can be prepared by chemical or electrochemical methods and can be chemically tailored to fit a wide range of technological purposes. Their reversible change from a metallic conductor to a semiconductor material by electrochemical doping/undoping enables the application of these materials in different electronic devices, including photovoltaic and photoelectrochemical cells [40]. Several studies have demonstrated the photoeffects produced by illuminating the heterojunction formed at the interface between an electrolyte and a conducting polymer in its semiconducting state, such as polyaniline, [41–44], polypyrrol [43,45,46] and polythiophene [47–50]. The energy conversion is low in comparison to the junctions using inorganic materials, however, the energy conversion is far from the theoretical limit and the possibility to produce inexpensive and flexible devices with different sizes and shapes makes this research very attractive.

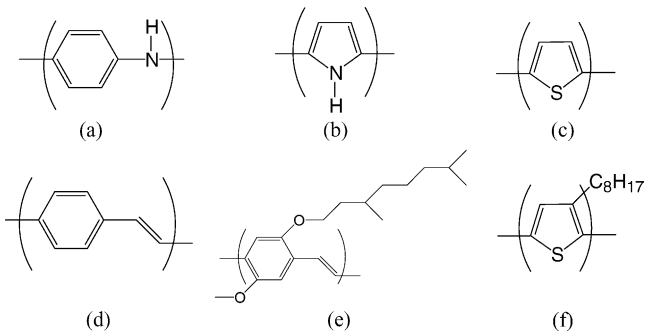

Fig. 3. Chemical structure of the repeating units of some intrinsically conducting polymers that present hole transport properties.

The first requirement for a conducting polymer to act as HTM in a DSSC relies on its wetability. Polymers cast from solutions must penetrate into the pores of the nanoparticles and should form a good contact with the adsorbed sensitizer. As a consequence the polymer molar mass is crucial in order to achieve efficient pore filling. Several other requirements must be also fulfilled to produce efficient solid-state DSSC using conducting polymers as HTM, as discussed by Gebeyehu et al. [51]: the polymeric material must be highly transparent in the spectral range of dye absorption; the polymer HTM should be deposited onto the TiO_2 film without dissolving or degrading the dye monolayer; the excited state energy of the sensitizer (S^*) must be higher than the TiO_2 conduction band edge and the sensitizer ground state energy must be below the upper edge of the valence band of the p-type conducting polymer. This is required for electron transfer from the excited dye molecule to the conduction band of TiO_2 and hole transfer from TiO_2 to the valence band of the HTM. The hole mobility in the polymeric HTM must be sufficiently high to prevent charge recombination.

Gebeyehu et al. have successfully applied polytiophene derivatives as HTM in DSSC. Solid-state devices using poly(3-octylthiophene) as HTM presented I_{SC} and V_{OC} values of 450 μA cm^{-2} and 0.65 V at 80 mW cm^{-2} [51].

However, the conversion efficiencies reported for all DSSC assembled with conducting polymers as HTM are low in comparison to the cells using a liquid or polymer electrolyte [52–56], mainly due to the incomplete filling of the TiO_2 nanopores by the HTM, which leads to poor electronic contact between the dye molecules and the hole conductor. In fact, organic molecular HTM, possessing a better wettability, present higher energy conversion efficiencies. The authors reported an efficiency of 2.6% for a DSSC assembled with the amorphous HTM Spiro-OMeTAD. An increase in the cell output was achieved due to inhibition of interface charge recombination adding 4-*tert*-butylpiridine and a lithium salt, $Li[CF_3SO_2]_2N$ [34].

Other parameters could also account for low energy conversion:

(i) The high charge recombination rate at the TiO_2–HTM interface between the electrons in the conduction band/trap states and the oxidized HTM. A charge recombination reaction can occur between the electrons present in the TiO_2 conduction band/trap states Eq. (10) or with the oxidized HTM (this process is also referred to dark current, Eq. (11). Bach et al. determined the rate of the re-reduction reaction between the HTM and the oxidized dye Spiro-MeOTAD by transient absorption spectroscopy. According to these authors this process is relatively fast, occurring on a picosecond timescale [57]. Thus, the recombination reaction between the electrons and the oxidized HTM is expected to constitute the major loss mechanism in this cell [37]. In fact, Rau and coworkers showed that this charge recombination explains the low photovoltage (100–200 mV difference in comparison to the liquid electrolyte) obtained in DSSC using HTM [58].

(ii) The low conductivity of the hole conductor itself. Conducting polymers exhibit low hole mobility in comparison to inorganic materials. This is assigned to disorder characteristics of these materials giving rise to a broad distribution of trap states in the material. One of the reasons to use inorganic HTM such as CuI or CuSCN relates on their increased hole mobility compared to amorphous polymeric HTM. In fact, DSSC assembled using inorganic HTM showed high efficiencies, with energy conversions approaching 4% [59–65]. DSSC assembled using CuI and 1-methyl-3-ethyl-imidazolium thiocyanate as crystal growth inhibitor have exhibited $I_{SC} \sim 12\,mA\,cm^{-2}$ and an initial overall efficiency of 3.8% [59].

(iii) Low connectivity between the HTM and the hole collector electrode. Yanagida and collaborators have demonstrated the use of polypyrrol (PPy) polymerized in situ on nanoporous TiO_2 as HTM. The first devices showed low energy conversion (~0.1%) [66]. More recently, they reported an increase in cell efficiency using carbon paste deposited on top of a platinum electrode. A device with the configuration TiO_2/dye/PPy/C-Pt exhibited $I_{SC} = 104\,\mu A\,cm^{-2}$, $V_{OC} = 0.716\,V$ and an overall efficiency of 0.62% [67].

In general, many conducting polymers in their undoped semiconducting state are electron donors upon photoexcitation, with high band gap energies (E_g). Therefore, these materials may replace, in principle, the dye and the liquid electrolyte, bringing together the function of sensitizer and HTM in a single material. Thus, in principle, the sensitizer dye can be replaced by a conducting polymer, combining the function of charge transport and light absorption. The capability of the conducting polymers to act as TiO_2 sensitizer has already been demonstrated for poly(phenyl vinylene), polythiophene and poly(*o*-methoxyaniline) [68–72], showing that TiO_2 acts as an efficient electron acceptor. Several groups have reported the use of conducting polymers as both sensitizer and hole conductor material, however, the efficiencies are lower than the cells using a combination of Ru(II) bipyridine complexes as dye and a conducting polymer as HTM [51,54,55].

To act as an efficient sensitizer, the conducting polymer should present a high exciton diffusion length, to decrease charge recombination, and a highly efficient electron transfer from the polymer layer into the TiO_2 conduction band. In fact, one of the major drawbacks of using polymer films in photoelectrochemical and photovoltaic devices is their small exciton diffusion length. This parameter determines the extent of exciton diffusion, prior to geminate recombination. For an efficient charge separation, the exciton diffusion length should be greater than the distance between the electron acceptor and donor molecules. According to Savenije et al., the exciton diffusion path length was 20 nm for a spin-coated film [68]. Other reports estimated this parameter in the range of 5–20 nm [73,74]. The photoinduced charge transfer from the conjugated polymer poly(*p*-phenylene vinylene), PPV, into TiO_2 was estimated to reach 60%, when the thickness of the polymer film is below the polymer exciton diffusion length of ca. 20 nm [71]. This estimated quantum efficiency for electron transfer is in agreement with the incomplete filling of the pores of the TiO_2 films. This problem is the major drawback in these cells because parts of the polymer chains remain isolated and, therefore some fractions of the photoexcited charge carriers do not reach the interface with TiO_2, where charge separation occurs [75]. Recently, Janssen and co-workers reported a new hybrid bulk heterojunction using a PPV derivative, poly[2-methoxy-5-(3′,7′-dimethyl-octyloxy)-*p*-phenylene vinylene], MDMO-PPV, blended with TiO_2 [76]. Time-resolved photoluminescence experiments have indicated a sub-picosecond charge transfer between the conducting polymer and TiO_2.

5. Solid-state electrolytes

The development of DSSC using polymer-based electrolytes has created a misunderstanding in the literature. For

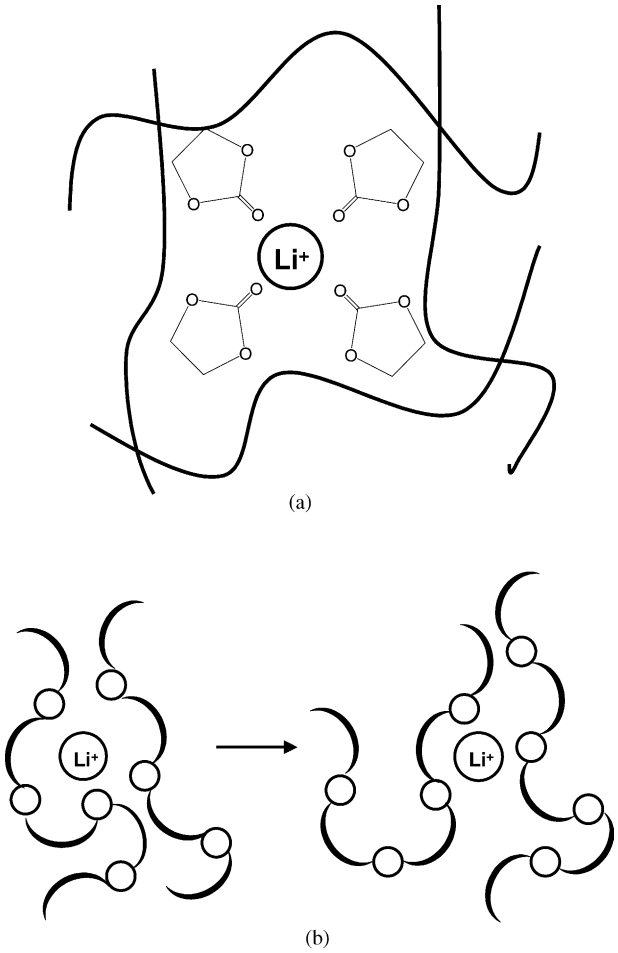

Fig. 4. Schematic representation of the ionic transport in a polymeric matrix. (a) Gel polymer electrolyte: lithium cations are dissociated by the organic solvent and are transported through the free volume or micropore of the polymer matrix and the liquid electrolyte. (b) Polymer electrolyte: lithium cations are dissociated by the polymer matrix and transported through Lewis acid–base interactions in the free volume of the matrix, assisted by polymer segmental motion.

this reason we will divide this topic into two main categories: the use of a *gel electrolyte*, that gives rise to a *quasi-solid-state DSSC*, and the use of a *pure polymer electrolyte* (without solvent), giving a *solid-state DSSC*. Fig. 4 shows a schematic representation of the structure of a gel and a solid polymer electrolyte, emphasizing the mechanism for ionic transport in both systems. In this section, we will outline some background research using polymers as electrolytes and focus on the more recent advances in this field.

5.1. Gel electrolytes

Before introducing the research involving solvent-free polymer electrolyte and gel electrolyte applied to DSSC, it is important to clarify some aspects involving "plasticized electrolytes" and polyelectrolytes. Plasticized electrolytes are a class of electrolyte that are on the boundary between gel and polymer electrolytes. The plasticizer, usually a low molar mass polyether (e.g. polyethylene glycol) or a polar organic solvent (e.g. ethylene carbonate or propylene carbonate) is introduced in small fractions into the polymeric matrix to lower the glass transition temperature of the polymer and increase its segmental mobility. The plasticizer introduces a degree of disorder in the crystalline phase because it remains between the adjacent polymer chains, reducing the polymer–polymer chain interaction and increasing the free volume of the system. PEO-plasticized electrolytes reach high ionic conductivity, approaching $10^{-3}\,S\,cm^{-1}$ at 25 °C [77]. Polyelectrolytes constitute a class of polymers in which the anion is attached to a polymer backbone via chemical bonds, thus the transport properties are assigned to the mobile cations.

Polymer gels have been actively developed as highly conductive electrolyte material for lithium secondary batteries and fuel cells [78]. By definition, a polymeric gel is defined as a system that consists of a polymer network swollen with a solvent [79,80]. Owing to their unique hybrid network structure, gels have both the cohesive properties of solids and the diffusive transport properties of liquids. Polymer gel electrolytes are characterized by a high ambient ionic conductivity but poor mechanical properties, when compared with pure polymer electrolytes. Gel electrolytes are usually obtained by incorporating a large amount of a liquid plasticizer and/or solvent (containing the desired ionic salts) into a polymer matrix, giving rise to a stable gel with a polymer host structure. When gelation occurs, a dilute or more viscous polymer solution is converted into a system of infinitive viscosity, a gel. The polymer or oligomer that form this stable network is often named a "gelator", because it solidifies the liquid phase. In order to improve the mechanical properties of the gel, components that can be cross-linked and/or thermoset may also be incorporated into the gel electrolyte formulation. Thus, gels can be obtained as a result of either a chemical or a physical cross-linking process. Chemical or covalent cross-linking leads to the formation of irreversible gels. By contrast, the gel network formed via physical cross-linking is called an "entanglement network". There are several polymer matrices used to obtain polymer gels; the most investigated being poly(ethylene oxide), poly(acrylonitrile), poly(vinyl pyrrolidinone), poly(vinyl chloride), poly(vinylidene carbonate), poly(vinylidene fluoride) and poly(methyl methacrylate).

The first attempt to use a gel electrolyte in a quasi-solid-state DSSC was done by Cao et al. using a mixture of poly(acrylonitrile), ethylene carbonate, propylene carbonate, acetonitrile, and a specific concentration of NaI [81]. The gel was obtained after 3 days of gelation. The energy conversion efficiency for cells assembled with this sort of gel network polymer is low in comparison to "liquid cells", attributed to the low penetration of the polymer network into the TiO_2 film [81–83].

In order to increase the wettability of the gel electrolyte into the oxide films, Yanagida and collaborators introduced the use of low molar mass gelators to solidify the liq-

uid electrolyte [84]. These gelators form thermoreversible physical gels from a variety of organic liquids at very low concentration. The use of these low molar mass gelators allows the complete filling of the TiO_2 nanopores by the gel network. Using this approach, a mixture containing low molar mass gelators based on amino acid derivatives, solvent–plasticizers and ionic salts is heated to 100–140 °C and the resulting fluid electrolyte is introduced in the cell. After the injection of the fluid electrolyte, cooling to room temperature carries out gelation of the cell. DSSC assembled using this gelator showed efficiencies up to 3.0% at AM 1.5 conditions [84]. The best performance was reported for a cell using gelators containing amide and urethane groups [85–87]. The optimized quasi-solid-state DSSC showed values of $V_{OC} = 0.67$ V, $I_{SC} = 12.8$ mA cm^{-2} and an overall efficiency of 5.91% under AM 1.5 conditions [85]. The gelation of the electrolyte also remarkably influences cell stability, improving its durability by suppressing solvent evaporation.

Improvements in the performance of these quasi-solid-state DSSC can be achieved using room temperature molten salts (RTMS). RTMS such as imidazolium salts and pyridinium salts have superior properties due to their chemical stability, non-volatility, non-flammability and high ionic conductivity at room temperature. Another attraction issue is that RTMS have low melting point and do not undergo crystallization like alkaline iodide salts, due to the low solubility of the latter in organic solvents. However, the use of RTMS alone produces cells with low performance. For instance, DSSC assembled with low temperature molten salts based on methyl-hexyl-imidazolium iodide exhibited I_{SC} values ranging from 1 to 6 mA cm^{-2} and efficiencies of 0.4–2%, depending on the viscosity of the medium. Studies revealed a slow diffusion of I^-/I_3^- redox species due to the high viscosity of these molten salts; decreasing the viscosity of the medium caused an improvement in the performance of the solar cell [88,89].

Yanagida and co-workers reported 5.0% efficiency (AM 1.5 conditions) for a DSSC assembled using room temperature molten salts based on 1-alkyl-3-methylimidazolium iodide (alkyl: C_3–C_9) combined with a low molar mass gelator [86,87]. The cells were submitted to light and thermal stresses and showed good stability. The devices assembled with the RTMS maintained 70% of the initial efficiency after 1000 h at 85 °C.

Hayase and co-workers in collaboration with Toshiba Corporation have prepared polymer gel electrolytes using gelators, followed by a cross-linking reaction, giving rise to stable cross-linked gels [90,91]. This was the first successful report with chemically cross-linked polymers. However, this method could not be used for DSSC because iodide inhibits the cross-linking reactions [92]. A gel electrolyte containing 1-methyl-3-propyl imidazolium iodide (MPII) as RTMS, a cross-linking agent and a gelator (referred as a liquid pre-gel) was injected into an already set DSSC. The gelation was carried out in the cell by heating at 80 °C. This induced the formation of a three-dimensional covalent polymer network in the cell [90,91]. These cells exhibited current densities of 8–10 mA cm^{-2} and 7.3% efficiency [93].

Quasi-solid-state DSSC assembled with a polymer gel electrolyte based on a fluorinated copolymer, poly(vinylidene fluoride-*co*-hexafluoropropylene) (PVDF–HFP) combined with RTMS also exhibited high overall energy conversion efficiency. Grätzel and co-workers reported cells yielding an efficiency of 5.3% (AM 1.5 conditions) [94]. Interestingly, an analogous cell using a liquid electrolyte showed similar performance, indicating that the copolymer has no adverse effect on the conversion efficiency. Improvements in cell performance and stability were achieved using an amphiphilic bipyridyne ruthenium dye and PVDF–HFP to solidify a 3-methoxyproprionitrile-based liquid electrolyte [95]. The cell exhibited $I_{SC} = 12.5$ mA cm^{-2}, $V_{OC} = 0.73$ V and a conversion efficiency of 6.1% at 100 mW cm^{-2}. The efficiency was maintained at 94% of its initial value after exposure for 1000 h at 80 °C.

Further progress occurred when nanocomposite gel electrolytes were applied to DSSC using semiconductor nanoparticles to solidify the liquid phase composed of room temperature molten salts (MPII) [96–98]. This procedure produced solar cells with overall efficiencies close to 7.0% [96].

Despite their high conversion efficiency, quasi-solid-state DSSC still exhibit current density values lower than DSSC using the conventional liquid electrolyte. Yanagida and co-workers investigated charge transport properties in the cells containing gel electrolytes [85]. They showed that the gelation process did not significantly influence the charge transport in the electrolyte. However, the diffusion of the iodide ions is ca. one quarter of that observed in acetonitrile [85]. These transport limitations have several implications for electron transport into the cell. It was confirmed that dye regeneration competes effectively with charge recombination between the electrons injected into the conduction band/trap states and the oxidized dye [87,95,99]. In addition, the slow diffusion of I_3^- gives rise to accumulation of these species in the counter electrode, limiting I_{SC} values and increasing the dark current [87]. Another problem involving polymer gels relates to their stability. It is well known that gel systems are thermodynamically unstable. They may undergo solvent exudation upon long storage, especially under open atmospheric conditions, decreasing their ionic conductivity and, as a consequence, cell efficiency. High temperature conditions also have a detrimental effect on cell performance because solvent with a high vapor pressure can affect the sealing conditions.

5.2. Polymer electrolytes

Interesting results were also obtained for solid-state DSSC assembled with solvent-free polymer electrolytes. Before presenting an overview of the results obtained with a solid-

state DSSC using polymer electrolytes, it is worthwhile to consider some properties of this kind of electrolyte.

The polymer-based material is generally produced in a thin-film configuration by casting or spin-coating techniques. Polymer electrolytes are composed by alkaline salts (e.g. lithium or sodium salts) dissolved in a high molar mass polyether host (e.g. poly(ethylene oxide) (PEO) or poly(propylene oxide) (PPO)) [100]. In polymer electrolytes, the polymer matrix should be an efficient solvent for the salt, capable of dissociating it and minimizing the formation of ion pairs. The solubility of the salt relies on the ability of the electron donor atoms in the polymer chain to coordinate the cation through a Lewis type acid–base interaction. This interaction also depends on the lattice energy of the salt and the structure of the host polymer. The mechanism for ionic motion in polymer electrolytes results from a solvation–desolvation process along the chains that occurs predominantly in the amorphous polymer phase (see Fig. 4). Since the ionic motion is strictly correlated with the segmental motion of the polymer chains, the ionic conductivity increases with increasing chain mobility. The ionic conductivity is also a function of the number of charge carriers in the polymer matrix. However, above a limiting high salt concentration the segmental motion of the polymer chains is reduced due to an "ionic cross-linking" which decreases ionic conductivity [101].

Specifically for PEO, the repeating unit (–CH_2–CH_2–O–) seems to present a favorable arrangement for effective interaction of the free electron pair on the oxygen with the alkali metal cations. This occurs because the PEO chains are capable of adopting a helical conformation with an oxygen-lined cavity that presents ideal distances for oxygen–cation interactions. Due to this interaction, the ionic conductivity is associated with the concentration ratio of oxygen in the ethylene oxide repeating units and the cations of the salt, $\eta_{EO} = [O]_{EO}/[cation]$. PEO is characterized by a low glass transition temperature ($T_g = -50\,^{\circ}C$), but the regular structure favors a high degree of crystallinity (~80%), with its melting point at $T_f = 65\,^{\circ}C$. Thus solvent-free PEO–salt complexes exhibit conductivity in the range from 10^{-8} to $10^{-4}\,S\,cm^{-1}$ at temperatures between 40 and 100 °C, which limits practical applications at room temperature. To obtain a more amorphous polymer at ambient temperature, it is necessary to introduce a certain degree of disorder in the structure. This is achieved by using blends [102–104], copolymers, comb-branched polymers and cross-linked networks [105]. All these modifications have been achieved either by reducing the crystallinity of the polymer or by lowering the glass transition temperature. Also, the incorporation of nano-sized silica or other oxides has produced interesting results [106,107].

Promising results have been obtained by our group using a polymer electrolyte based on the copolymer poly(ethylene oxide-*co*-epichlorohydrin), $P(EO–EPI)_{84:16}$, produced by Daiso Co., Ltd. (Osaka, Japan), complexed with sodium or lithium iodide salts [108,109]. The characterization of

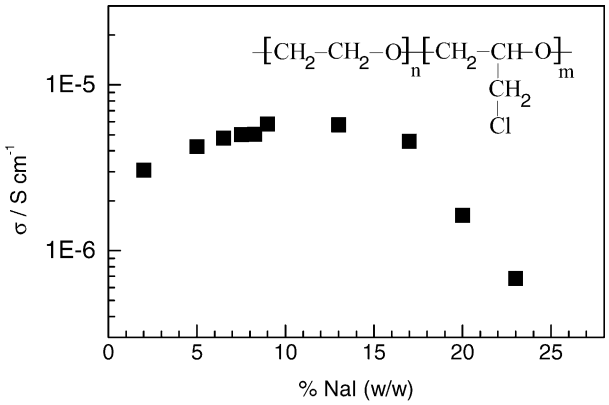

Fig. 5. Variation of the ionic conductivity of the polymer electrolyte $P(EO–EPI)_{84:16}$ with the concentration of NaI, expressed as a function of the ratio $\eta_{EO} = [O]_{EO}/[Na]$. Measurements performed in a dry box at 26 °C. The repeating unit of poly(ethylene oxide-*co*-epichlorohydrin), where *n* and *m* are 0.84 and 0.16, respectively, $P(EO–EPI)_{84:16}$, is also shown.

the polymer electrolytes consisting of $P(EO–EPI)_{84:16}$ with different concentrations of NaI and I_2 was performed by measurements of ionic conductivity, differential scanning calorimetry (DSC) and thermogravimetry (TGA) [110]. Fig. 5 shows the variation of the conductivity of the polymer electrolyte with the concentration of NaI, expressed as a function of $\eta_{EO} = [O]_{EO}/[Na]$ and determined in a dry box at 26 °C. With the increasing number of charge carriers, the ionic conductivity initially increases with the NaI concentration. However, after reaching a maximum value, it decreases because higher salt concentrations lower the segmental motion of the polymeric chains. For this system, the highest conductivity, $5.6 \times 10^{-6}\,S\,cm^{-1}$, was obtained at $\eta_{EO} = 24$, which corresponds to 9% (w/w) NaI concentration [110].

Considering these results, DSSC were assembled using a polymer electrolyte consisting of $P(EO–EPI)_{84:16}$ containing 9% NaI and 0.9% I_2 (w/w). Fig. 6 shows a schematic representation of all the steps involved in the assembly of a solid-state DSSC using a polymer electrolyte. Usually, the cells were prepared by spreading the surface of glass–FTO electrodes with an aliquot of a TiO_2 suspension using a glass rod (adhesive tape was used as spacer of ca. 40–50 μm thickness), followed by heating at 450 °C for 30 min. The glass-FTO|TiO_2 electrodes were immersed overnight (ca. 16 h) in a $\sim 1.5 \times 10^{-4}\,mol\,L^{-1}$ ethanol solution of Ru^{II}(2,2′-bipyridyl-4,4′-dicarboxylate)$_2$-$(NCS)_2$ ("N3 dye"), rinsed with ethanol and dried. Afterwards, a film of the polymer electrolyte was deposited onto the sensitized electrodes by casting, using a solution of $P(EO–EPI)_{84:16}$ with NaI and I_2 in acetone. The assembly of the cells was completed by pressing the Pt counter electrode against the sensitized electrode coated with the polymer electrolyte. The active area of the cells was typically $1\,cm^2$. Variations in this procedure were made by using different TiO_2 suspensions, slight variations in the composition of the

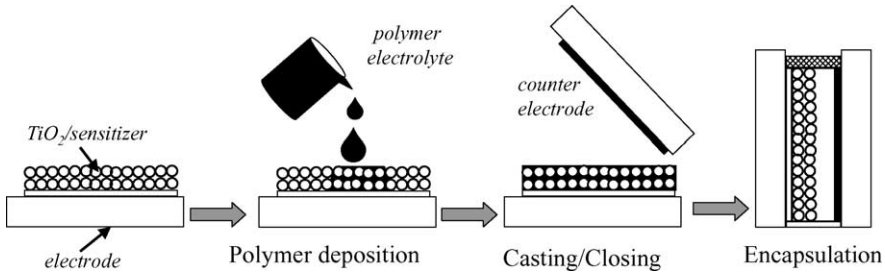

Fig. 6. Schematic representation of the steps involved in assembling a solid-state DSSC using a polymer electrolyte.

polymer electrolyte, including eventual addition of a small concentration of LiI, as well as the use of different counter-electrodes. The counter-electrodes consisted of a thin Pt film deposited onto glass–FTO electrodes by sputtering or by thermal deposition from a solution of hexachloroplatinic acid in isopropanol heated at 385 °C for 20 min.

The performance exhibited by an N3 dye-sensitized TiO_2 solar cell with P(EO–EPI)/I_3^-/I^- polymer electrolyte and using glass–FTO electrodes can be evaluated in Fig. 7, which shows some typical *I–V* curves obtained under different light intensities. The inset exhibits the photocurrent action spectra, obtained by irradiating the cell from the glass–FTO|TiO_2 side (SE) and from the counter-electrode side (EE). The IPCE curves show maximum photocurrent values at approximately 520 nm (51 and 40% for SE and EE irradiation), corresponding to the maximum in the N3 dye absorption spectrum. The best energy conversion efficiency obtained was $\eta = 2.6\%$ under 10 mW cm^{-2} (1.6% under 100 mW cm^{-2}). However, comparison with results reported in the literature is not straightforward, since the area of the cells (not always reported) can be very different. Due to an increase in the series resistance the efficiency of a DSSC decreases considerably when the cell area is enlarged. This effect can be more important when using polymer electrolytes. The V_{OC} values are high ($V_{OC} = 0.82$ V) and could result from interactions of the basic copolymer with the acid sites of the TiO_2 surface, which could suppress part of the dark current. However, the values of photocurrent ($I_{SC} = 4.2$ mA cm^{-2} at 100 mW cm^{-2}) and overall efficiency are lower than those exhibited by DSSC assembled with liquid electrolytes, and both decreased with increasing light intensity. This characteristic of the DSSC with polymer electrolytes is related to the lower mobility of I^-/I_3^- species in this medium, which retards the kinetics of the dye regeneration reaction in Eq. (4) [99].

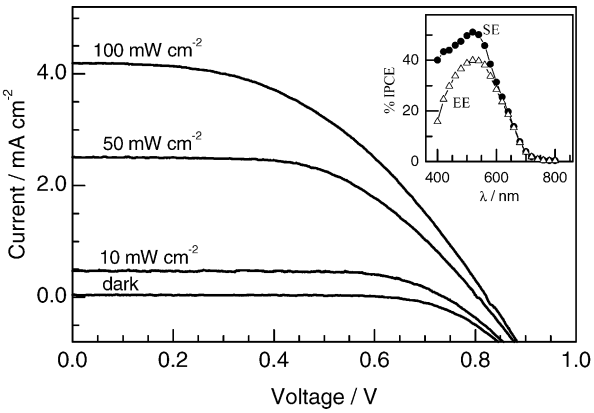

Fig. 7. Typical *I–V* curves obtained at different light intensities for a N3 dye-sensitized TiO_2 solar cell assembled with P(EO–EPI)/I^-/I_3^- polymer electrolyte. In the insert, photocurrent action spectrum determined by irradiating the cell from the FTO–TiO_2 side (SE) or counter-electrode side (EE).

Transient absorption spectroscopy measurements were done to confirm the above-mentioned assumption. The kinetics of dye cation reduction by iodide ions in the polymer electrolyte medium exhibited a half life ($\tau_{1/2}$) of 50 μm, which is two–three orders of magnitude slower than that observed in an acetonitrile-based electrolyte. As previously discussed, the kinetics of this reaction can also affect other kinetic processes that occur during cell operation, increasing, for instance, the probability of charge recombination reactions of injected electrons with the dye cation and with triiodide, lowering cell efficiency. This effect may become even more critical for high light intensities, when the demand of charge carrier transport between the electrodes is higher [99].

This light intensity-dependent performance of the cell can be derived from the *I–V* curves. To fit the *I–V* curves exhibited by these solar cells it is necessary to use a two-diode model, with an additional term that express a light dependent recombination current. Good fits were obtained using this model for all the curves presented in Fig. 7. Among other parameters obtained from the fit, the series resistance was estimated as $R_S = 60\ \Omega$. This high R_S is consistent with the ionic conductivity of the polymer electrolyte [99].

Using electrochemical impedance spectroscopy it is possible to evaluate the series resistance and observe that this parameter also depends on the characteristics of the TiO_2 photoelectrode, including the method used for preparing the TiO_2 film and the substrate [18,19]. For instance, the R_S values for different solid-state DSSC assembled with glass–FTO|TiO_2 photoelectrodes were 35–50 Ω, which is the same order of magnitude as the value estimated from fitting the *I–V* curves. With the flexible cells assembled with PET–ITO electrodes we measured $R_S \sim 400\ \Omega$, which can be related to the poor electrical contact between the

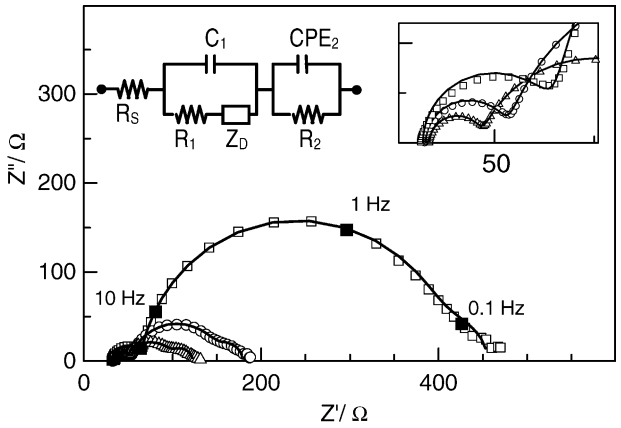

Fig. 8. Nyquist representation of the impedance data obtained for a solid-state N3 dye-sensitized TiO_2 solar cell prepared with P(EO–EPI)/I^-/I_3^- polymer electrolyte. Experimental data are represented by symbols and the solid lines correspond to fits obtained with Boukamp software using the circuit presented in figure. The insert presents the magnification of the high frequency region.

particles in the TiO_2 network, due to the low annealing temperature. Also, all the impedance spectra determined for the DSSC assembled with polymer electrolytes exhibited a low frequency response, which can be associated with diffusion processes in the electrolyte.

Fig. 8 shows some typic Nyquist diagrams from the impedance spectra, obtained using a small perturbation (±10 mV) over the V_{OC} of the cell and under different light intensities, for a N3 dye-sensitized TiO_2 solar cell assembled with P(EO–EPI)/I^-/I_3^- and using glass–FTO electrodes. Experimental data are represented by symbols while the solid lines correspond to the fit obtained with Boukamp software using the equivalent circuit R_S [C_1 (R_1Z_{Dif1})] (R_2CPE_2), depicted in the insert. In this circuit, the symbols R and C describe resistance and capacitance, respectively; Z_{Dif} accounts for a finite-length Warburg diffusion, and CPE is the symbol for the constant phase element. The insert also shows the magnification of the high-frequency region. In general, the impedance spectra of these solid-state solar cells also depend on light intensity. In the dark (curve not shown), the solar cell presented high impedance and the time constants were not well defined. Under illumination, three semicircles could be identified in the Nyquist diagrams of the EIS spectra. At high frequencies, the response associated with a small capacitance (∼12 μF cm^{-2}), which was almost independent of illumination, was attributed to the Pt|electrolyte interface (C_1 and R_1 elements). The response at medium frequencies, related to a high capacitance that strongly depends on light intensity, was attributed to the TiO_2|electrolyte interface (R_2CPE_2 elements), because an accumulation of electrons and redox species is expected at this interface under open circuit conditions. The response at low frequencies was associated to diffusion processes in the electrolyte, considering the lower mobility of the I_3^-/I^- species in the polymer electrolyte.

The general behavior of all the spectra determined by the authors for different cells was quite similar, but the impedance of the flexible cells was higher than that exhibited by cells prepared using glass electrodes [18]. It is interesting to compare the results obtained from *I–V* curves and the EIS measurements for cells prepared using polymer electrolytes and glass or flexible ITO/PET electrodes. Both cells exhibited similar V_{OC} values, but the flexible cell presented I_{SC} values 10 times lower and R_S values 10 times larger, in comparison with the cell assembled with glass electrodes. The stability of these flexible cells was also investigated over 50 days, illuminating the cell at 10 and 100 mW cm^{-2} at 25 °C. In agreement with the decrease in photocurrent and efficiency values observed from *I–V* curves, EIS measurements revealed an increase of R_S with time. Thus, it can be inferred that the high R_S, which increases with time, is responsible for the lower performance and stability exhibited by the flexible cells.

Current studies by the authors include the characterization of a new copolymer, consisting of 78% ethylene oxide and 22% diethylene glycol glycidyl methyl ether, poly(EO–DGME)$_{78:22}$ (also provided by Daiso Co. Ltd., Osaka). Preliminary studies reveal that this copolymer complexed with I_3^-/I^- can be applied as an efficient polymer electrolyte in DSSC. This new polymer matrix allows the dissolution of a higher concentration of NaI, which can enhance the performance of the solar cell [111]. We are also investigating new alternative methods for depositing TiO_2 films having larger pores to improve the ionic transport inside the nanoporous TiO_2.

Up to the present, the best results reported for a solid-state DSSC were obtained by Falaras and co-workers using a composite of poly(ethylene oxide)/TiO_2 and I_3^-/I^- as solid polymer electrolyte [112]. In this study, TiO_2 nanoparticles were introduced in the polymer electrolyte as fillers, decreasing PEO crystallinity and, as a consequence, increasing the ionic conductivity (∼ 10^{-5} S cm^{-1}). It has been proposed that the Lewis acid–base interactions between the surface hydroxyl groups of the nanoparticles and the oxygen of the PEO chains also contribute to increase salt dissociation. The cell presented an energy conversion of 4.2% under 65 mW cm^{-2} (active area 0.25 cm^2).

As a general rule, all the DSSC assembled with polymer electrolytes exhibited lower efficiency than the cells assembled using liquid electrolytes. This effect is caused by the lower ionic mobility of the I^-/I_3^- species in the polymeric medium, which affects the kinetics of all the processes involved in cell operation. But, in spite of the lower performance, the benefits obtained by the replacement of the liquid electrolyte can be worthwhile. Another issue is the great potential to be developed in the field of polymers as electrolyte: the search for higher ionic conductivities (and transport properties), stability improvement and new materials.

In general, both solid-state and quasi-solid-state DSSC prepared using polymer electrolytes and polymer gel electrolytes, respectively, on glass or flexible electrodes present

lower current densities but higher photovoltage values, even under low illumination conditions, opening the possibility to use these cells in conditions where low light intensity is present (e.g. indoor applications).

6. Final remarks

Dye-sensitized TiO_2 solar cells efficiently convert solar energy into electricity using low cost and easy-to-make materials, becoming a promising alternative to classical photovoltaic devices based on inorganic semiconductor technology. In addition to practical interest as an effective alternative energy source, these devices are also very fascinating systems from a scientific point of view, in which electrical energy is obtained from an elegant excitation–charge injection–redox process. This is a result of a successful combination of materials, usually consisting of a dye-sensitized nanocrystalline TiO_2 film, an electrolyte with a redox couple and a counter-electrode.

The overall efficiency in energy conversion depends critically on the individual properties of the constituents of the cell and their successful interactions. Enhancement of their performance involves understanding and controlling the properties of each component, and knowing how they affect the related processes in energy conversion.

Plastic materials have recently been applied to DSSC to overcome problems that have hampered widespread practical use. For instance PET–ITO based electrodes can substitute glass–FTO electrodes, improving the flexibility and impact resistance of a DSSC. Liquid electrolytes are volatile and may leak if the cell is not properly sealed. Their replacement by polymer electrolytes solves both problems with the additional advantage that they act as a binder for the electrodes. Intrinsically conducting polymers have also been used as hole transport materials in DSSC with promising results. The lower efficiency encountered in the devices assembled with plastic components, in comparison to DSSC using glass electrodes and liquid electrolytes, can in part be related to limited charge transport (both electronic and ionic) and to high resistivity of the plastic materials. However, the recent introduction of polymer materials in DSSC opens up an interesting research field with a high potential. Polymeric materials are less expensive, lighter and consume less energy for their large scale production, making these cells more environmental friendly.

Acknowledgements

The authors acknowledge financial support from FAPESP and PRONEx/CNPq and thank Daiso Co. Ltd., Osaka, Japan, for providing the polymer electrolytes. We also thank Prof. James Durrant (Imperial College, London) and Prof. Luiza De Cola (University of Amsterdam) for collaboration in the transient absorption spectroscopy measurements and helpful discussions. We also want to express our gratitude to Prof. Carol H. Collins, who has corrected our manuscripts for the last 25 years.

References

[1] B. O'Reagan, M. Grätzel, Nature 353 (1991) 373.
[2] M.K. Nazeeruddin, A. Kay, I. Rodicio, R. Humphrey-Baker, E. Muller, P. Liska, N. Vlachopoulos, M. Grätzel, J. Am. Chem. Soc. 115 (1993) 6382.
[3] A. Hagfeldt, M. Grätzel, Chem Rev. 95 (1995) 49.
[4] M. Grätzel, Curr. Opin. Colloid Interface Sci. (1999) 314.
[5] M. Grätzel, Measured under standard air mass 1.5 reporting conditions, PV calibration Laboratory of the National Energy Research Laboratory (NREL), Golden, CO, USA.
[6] A. Hinsch, J.M. Kroon, M. Späth, J.A.M. Van Roosmale, N.J. Bakker, P. Sommeling, N. Van der Burg, R. Kinderman, R. Kern, J. Ferber, C. Schill, M. Schubert, A. Meyer, T. Meyer, I. Uhlendorf, J. Holzbock, R. Niepmann, in: Proceedings of the 16th European Photovoltaic Solar Energy Conference and Exhibition, Glasgow, 2000.
[7] C. Longo, M.-A. De Paoli, J. Braz. Chem. Soc. 14 (2003) 889.
[8] W.A. Gazotti, G. Casalbore-Miceli, A. Geri, A. Berlin, M.-A. De Paoli, Adv. Mater. 10 (1998) 1522.
[9] M.-A. De Paoli, G. Casalbore-Miceli, E.M. Girotto, W.A. Gazotti, Electrochim. Acta 44 (1999) 2983.
[10] F. Pichot, S. Ferrere, R.J. Pitts, B.A. Gregg, J. Electrochem. Soc. 146 (1999) 4324.
[11] C.J. Brabec, F. Padinger, J.C. Hummelen, R.A.J. Janssen, N.S. Sariciftci, Synth. Met. 102 (1999) 8611.
[12] P.M. Sommeling, M. Späth, J. Kroon, R. Kinderman, J. van Roosmalen, in: Proceedings of the 16th European Photovoltaic Solar Energy Conference and Exhibition, Glasgow, 2000.
[13] W.A. Gazotti, A.F. Nogueira, E.M. Girotto, M.C. Gallazi, M.-A. De Paoli, Synth. Met. 108 (2000) 151.
[14] M.-A. De Paoli, D.A. Machado, A.F. Nogueira, C. Longo, Electrochim. Acta 46 (2001) 4243.
[15] H. Lindström, A. Holmberg, E. Magnusson, L. Malmqvist, A. Hagfeldt, J. Photochem. Photobiol. A: Chem. 145 (2001) 107.
[16] G. Boschloo, H. Lindström, E. Magnusson, A. Holmberg, A. Hagfeldt, J. Photochem. Photobiol. A: Chem. 148 (2002) 11.
[17] C. Longo, A.F. Nogueira, M.-A. De Paoli, H. Cachet, in: Z.H. Kafafi, D. Fichou (Eds.), Organic Photovoltaics II, Proceedings of the SPIE International Society for Optical Engineering, vol. 4465, San Diego, USA, 2002, p. 21.
[18] C. Longo, A.F. Nogueira, M.-A. De Paoli, H. Cachet, J. Phys. Chem. B 106 (2002) 5925.
[19] C. Longo, J.N. Freitas, M.-A. De Paoli, J. Photochem. Photobiol. A: Chem. 159 (2003) 33.
[20] J.R. Pichot, B. Pitts, A. Gregg, Langmuir 16 (2000) 5626.
[21] S. Balasubaramanian, K.G. Chittibabu, L. Li, L. Samuelson, J. Kumar, S. Tripathy, Photovoltaic Cells, US Patent Application (Provisional) (June 2001).
[22] R. Gaudiana, K. G. Chittibabu, Low Temperature Interconnection of Nanoparticles, US Patent Application (Provisional) (January 2002).
[23] R. Gaudiana, J. Macromol. Sci. A39 (2002) 1259.
[24] D.S. Zhang, T. Yoshida, H. Minoura, Adv. Mater. 15 (2003) 814.
[25] K. Kalyanasundaram, M. Grätzel, Coord. Chem. Rev. 177 (1998) 347.
[26] C.A. Kelly, G.J. Meyer, Coord. Chem. Rev. 211 (2001) 295.
[27] G. Oskam, B.V. Bergeron, G.J. Meyer, P.C. Searson, J. Phys. Chem. B 105 (2001) 6867.
[28] Z. Kebede, S.-E. Lindquist, Sol. Energy Mater. Sol. Cells 51 (1998) 291.

[29] Y. Liu, A. Hagfeldt, X.-R. Xiao, S.-E. Lindquist, Sol. Energy Mater. Sol. Cells 55 (1998) 267.
[30] C.A. Kelly, F. Fazard, D.W. Thompson, J.M. Stipkala, G.J. Meyer, Langmuir 15 (1999) 7047.
[31] D. Kuciauskas, M.S. Freund, H.B. Gray, J.R. Winkler, N. S Lewis, J. Phys. Chem. B 105 (2001) 392.
[32] M. Alebbi, C.A. Bignozzi, T.A. Heimer, G.M. Hasselmann, G.J. Meyer, J. Phys. Chem. B 102 (1998) 7577.
[33] S.A. Sapp, C.M. Elliot, C. Contado, S. Caramori, C.A. Bignozzi, J. Am. Chem. Soc. 124 (2002) 11215.
[34] J. Kruger, R. Plass, L. Cevey, M. Piccirelli, M. Gratzel, U. Bach, Appl. Phys. Lett. 79 (2001) 2085.
[35] J. Hagen, W. Schaffrath, P. Otschik, R. Fink, A. Bacher, H-W. Schmidt, D. Haarer, Synth. Met. 89 (1997) 215.
[36] K.R. Haridas, J. Ostrauskaite, M. Thelakkat, M. Heim, R. Bilke, D. Haarer, Synth. Met. 121 (2001) 1573.
[37] S.A. Haque, T. Park, A.B. Holmes, J.R. Durrant, Chem. Phys. Chem. 1 (2003) 89.
[38] R.W.T. Higgins, N.A. Zaidi, A.P. Monkman, Adv. Funct. Mater. 11 (2001) 407.
[39] S.E. Shaheen, C.J. Brabec, F. Padinger, T. Fromherz, J.C. Hummelen, N.S. Sariciftci, Appl. Phys. Lett. 78 (2001) 841.
[40] W.A. Gazotti, A.F. Nogueira, E.M. Girotto, L.Micaroni, M. Martini, S. das Neves, M.-A. De Paoli, in: H.S. Nalwa (Ed.), Handbook of Advanced Electronic and Photonic Materials, vol. 10, Academic Press, San Diego, 2000 (Chapter 2).
[41] J. Desilvestro, O. Haas, J. Chem. Soc., Chem. Commun. (1985) 346.
[42] P.K. Shen, Z. Tian, Electrochim. Acta 34 (1989) 1611.
[43] F.L.C. Miquelino, M.-A. De Paoli, E.M. Geniès, Synth. Met. 68 (1994) 91.
[44] S. das Neves, C.N. Polo da Fonseca, M.-A. De Paoli, Synth. Met. 89 (1997) 167.
[45] M. Kaneko, K. Okuzumi, A. Yamada, J. Electroanal. Chem. 183 (1985) 407.
[46] M. Martini, M.-A. De Paoli, Sol. Energy Mater. Sol. Cells 60 (2000) 73.
[47] S. Glenis, G. Horowitz, G. Tourillon, F. Garnier, Thin Solid Films 111 (1984) 93.
[48] S. Glenis, G. Tourillon, F. Garnier, Thin Solid Films 139 (1986) 221.
[49] L. Micaroni, M.-A. De Paoli, Sol. Energy Mater. Sol. Cells 43 (1996) 79.
[50] T. Yohannes, O. Ingänas, Synth. Met. 107 (1999) 97.
[51] D. Gebeyehu, C.J. Brabec, N.S. Sariciftci, D. Vangeneugden, R. Kiebooms, D. Vanderzande, F. Kienberger, H. Schindler, Synth. Mat. 125 (2002) 279.
[52] T.K. Däubler, I. Glowacki, U. Scherf, J. Ulanski, H.-H. Hörhold, D. Neher, J. Appl. Phys. 86 (1999) 6915.
[53] C.C. Wanser, H.-S. Kim, J.-K. Lee, Opt. Mater. 21 (2002) 221.
[54] S. Luzzati, M. Basso, M. Catellani, C.J. Brabec, D. Gebeyehu, N.S. Sariciftci, Thin Solid Films 403-404 (2002) 52.
[55] S. Spiekermann, G.P. Smestad, J. Kowalik, L.M. Tolbert, M. Gratzel, Synth. Metals. 121 (2001) 1603.
[56] G.P. Smestad, S. Spiekermann, J. Kowalik, C.D. Grant, A.M. Schwartzberg, J. Zhang, L.M. Tolbert, E. Moons, Sol. Energy Mater. Sol. Cells 76 (2003) 85.
[57] U. Bach, Y. Tachibana, J.-E. Moser, S.A. Haque, J.R. Durrant, M. Grätzel, D. Klug, J. Am. Chem. Soc. 121 (1999) 7445.
[58] G. Kron, T. Egerter, J.H. Werner, U. Rau, J. Phys. Chem. B 107 (2003) 3556.
[59] G.R.A. Kumara, S. Kaneko, M. Okuya, K. Tennakone, Langmuir 18 (2002) 10493.
[60] B. O'Reagan, D.T. Schwartz, J. Appl. Phys. 80 (1996) 4749.
[61] B. O'Reagan, D.T. Schwartz, S.M. Zakeeruddin, M. Grätzel, Adv. Mater. 12 (2000) 1263.
[62] K. Tennakone, G.R.R.A. Kumara, I.R. M Kottegoda, K.G.U. Wijayantha, V.P.S. Perera, J. Phys. D: Appl. Phys. 31 (1998) 1492.
[63] G.R.R.A. Kumara, A. Konno, K. Shiratsuchi, J. Tsukahara, K. Tennakone, Chem. Mater. 14 (2002) 954.
[64] B. O'Regan, F. Lenzmann, R. Muis, J. Wienke, Chem. Mater. 14 (2002) 5023.
[65] Q.B. Meng, K. Takahashi, X.T. Zhang, I. Sutanto, T.N. Rao, O. Sato, A. Fujishima, H. Watanabe, T. Nakamori, M. Uragami, Langmuir 19 (2003) 3572.
[66] K. Murakoshi, R. Kogure, Y. Wada, S. Yanagida, Chem. Lett. (1997) 471.
[67] T. Kitamura, M. Maitani, M. Matsuda, Y. Wada, S. Yanagida, Chem. Lett. (2001) 1054.
[68] T.J. Savenije, J.M. Warman, A. Goossens, Chem. Phys. Lett. 287 (1998) 148.
[69] P.A. van Hal, M.P.T. Christiaans, M.M. Wienk, J.M. Kroon, R.A.J. Janssen, J. Phys. Chem. B 103 (1999) 4352.
[70] A.F. Nogueira, M.-A. De Paoli, Synth. Met. 105 (1999) 23.
[71] T.J. Savanije, M.J.W. Vermeulen, M.P. De Haas, J.M. Warman, Sol. Energy Mater. Sol. Cells 61 (2000) 9.
[72] A.C. Arango, L.R. Johnson, V.N. Bliznyuk, Z. Schlesinger, S.A. Carter, H.-H. Horhold, Adv. Mater. 12 (2000) 1689.
[73] J.J.M. Halls, K. Pichler, R.H. Friend, S.C. Moratti, A.B. Holmes, Appl. Phys. Lett. 68 (1996) 3120.
[74] N.S. Sariciftci, Primary Photoexcitations in Conjugated Polymers: Molecular Exciton versus Band Model, World Scientific Publishers, Singapore, 1998.
[75] A.C. Arango, S.A. Carter, P.J. Brock, Appl. Phys. Lett. 74 (1999) 1698.
[76] P.A. van Hal, M.M. Wienk, J.M. Kroon, W.J.H. Verhees, L.H. Slooff, W.J.H. van Gennip, P. Jonkheijm, R.A.J. Janssen, Adv. Mater. 15 (2003) 118.
[77] Y. Ito, K. Kanehori, K. Miyauchi, T. Kudo, J. Mater. Sci. 22 (1987) 1845.
[78] K.M. Abraham, in: B. Scrosati (Ed.), Application of Electroactive Polymer, Chapman & Hall, London, 1993.
[79] S.B. Ross-Murphy, in: R.F.T. Stepto (Ed.), Polymer Networks—Principles of Their Formation, Structure and Properties, Blackie Academic and Professional, London, 1998.
[80] S. Megahed, B. Scrosati, Interface 4 (1995) 34.
[81] F. Cao, G. Oskam, P.C. Searson, J. Phys. Chem. 99 (1995) 17071.
[82] M. Matsumoto, H. Miyasaki, K. Matsuhiro, Y. Kumashiro, Y. Takaoka, Solid State Ion. 89 (1996) 263.
[83] Y. Reng, Z. Zhang, E. Gao, S. Fang, S. Cai, J. Appl. Electrochem. 31 (2001) 445.
[84] W. Kubo, K. Murakoshi, T. Kitamura, Y. Wada, K. Hanabusa, H. Shirai, S. Yanagida, Chem. Lett. 12 (1998) 1241.
[85] W. Kubo, K. Murakoshi, T. Kitamura, S. Yoshida, M. Hakuri, K. Hanabusa, H. Shirai, Y. Wada, S. Yanagida, J. Phys. Chem. B 105 (2001) 12809.
[86] W. Kubo, T. Kitamura, K. Hanabusa, Y. Wada, S. Yanagida, Chem. Commun. (2002) 374.
[87] W. Kubo, S. Kambe, S. Nakade, T. Kitamura, K. Hanabusa, Y. Wada, S. Yanagida, J. Phys. Chem. B 107 (2003) 4374.
[88] H. Matsumoto, T. Matsuda, T. Tsuda, R. Hagiwara, Y. Ito, Y. Miyazaki, Chem. Lett. (2001) 26.
[89] N. Papageorgiou, Y. Athanassov, M. Armand, P. Bonhôte, H. Pettersson, A. Azam, M. Grätzel, J. Electrochem. Soc. 143 (1996) 3099.
[90] S. Murai, S. Mikoshiba, H. Sumino, S. Hayase, J. Photochem. Photobiol. A: Chem. 148 (2002) 33.
[91] S. Mikoshiba, S. Murai, H. Sumino, S. Hayase, Chem. Lett. (2002) 918.
[92] K. Murakoshi, R. Kogure, Y. Wada, S. Yanagida, Solar Energy Mater. Sol. Cell 55 (1998) 113.
[93] S. Mikoshiba, H. Sumino, M. Yonetsu, S. Hayase, in: Proceedings of the 16th European Photovoltaic Solar Energy Conference, Glasgow, 2000.

[94] P. Wang, S. Zakeeruddin, I. Exnar, M. Grätzel, Chem. Commun. (2002) 2972.
[95] P. Wang, S. Zakeeruddin, J.E. Moser, M.K. Nazeeruddin, T. Sekigushi, M. Grätzel, Nat. Mater. 20 (2003) 402.
[96] P. Wang, S.M. Zakeeruddin, P. Comte, I. Exnar, M. Grätzel, J. Am. Chem. Soc. 125 (2003) 1166.
[97] E. Stathatos, P. Lianos, Adv. Mater. 14 (2002) 354.
[98] E. Stathatos, P. Lianos, S.M. Zakeeruddin, P. Liska, M. Grätzel, Chem. Mater. 15 (2003) 1825.
[99] A.F. Nogueira, M.-A. De Paoli, I. Montanari, R. Monkhouse, J. Nelson, J.R.J. Durrant, J. Phys. Chem. B 105 (2001) 7517.
[100] M. Armand, in: J.R. MacCallum, C.A. Vincent (Eds.), Polymer Electrolyte Reviews-1, Elsevier, London, 1987.
[101] M. Armand, Adv. Mater. 2 (1990) 278.
[102] W. Wieczorek, K. Such, Z. Florjanczyk, J. Przyluski, Electrochim. Acta 37 (1992) 1565.
[103] J. Li, M. Khan, Macromolecules 26 (1993) 4544.
[104] J.L. Acosta, E. Morales, J. Appl. Polym. Sci. 60 (1996) 1185.
[105] M. Cowie, in: J.R. MacCallum, C.A. Vincent (Eds.), Polymer Electrolyte Reviews-1, Elsevier, London, 1987.
[106] J.E. Weston, B.C.H. Steele, Solid State Ion. 7 (1982) 75.
[107] F. Croce, G.B. Appetecchi, L. Persi, B. Scrosati, Nature 394 (1998) 456.
[108] A.F. Nogueira, M.-A. De Paoli, Sol. Energy Mater. Solar Cells 61 (2000) 135.
[109] A.F. Nogueira, J.R. Durrant, M.-A. De Paoli, Adv. Mater. 13 (2001) 826.
[110] A.F. Nogueira, M.A. Spinacé, W.A. Gazotti, E.M. Girotto, M.-A. De Paoli, Solid State Ion. 140 (2001) 327.
[111] T.C. Ferreira Gomes, C. Longo, W. Gazotti, M.-A. De Paoli, Procc. XIII Simpósio Brasileiro de Eletroquímica e Eletroanalítica, Araraquara, 2002, pp. 99.
[112] T. Stergiopoulos, I.M. Arabatzis, G. Katsaros, P. Falaras, Nanoletters 2 (2002) 1259.